A Prenylated Protein-Specific Endoprotease in Rat Liver Microsomes That Produces a Carboxyl-Terminal Tripeptide†

Geeng-Fu Jang, Kohei Yokoyama, and Michael H. Gelb*

Departments of Chemistry and Biochemistry, University of Washington, Seattle, Washington 98195

Received December 29, 1992; Revised Manuscript Received April 5, 1993®

ABSTRACT: The maturation of proteins that contain the C-terminal sequence Cys-Ali-Ali-Xaa (where Ali is usually an aliphatic amino acid and Xaa is a number of different amino acids) involves the attachment of a farnesyl or geranylgeranyl group to the cysteine residue, proteolytic removal of the C-terminal three amino acids, and methylation of the prenylated cysteine α-carboxyl group. Two prenylated and radiolabeled peptides were prepared in order to detect the proteolysis step(s) in a cell-free system and to determine the reaction products. These peptides are ECB-NPFRQRRFFC(*S*-geranylgeranyl)AI[^{3}H]L and ECB-C(*S*-farnesyl)VI[^{3}H]S (ECB is an extended-chain biotin group) which are patterned after the C-termini of geranylgeranylated and farnesylated G protein γ-subunits. Incubation of these peptides with rat liver microsomes, but not cytosol, results in the production of radiolabeled dipeptides (I[^{3}H]L and I[^{3}H]S) and tripeptides (AI[^{3}H]L and VI[^{3}H]S) as the major products and smaller amounts of amino acids ([^{3}H]L and [^{3}H]S). A multitude of independent experiments shows that the dipeptides are produced from the tripeptides by secondary proteolysis. Although a portion of the [^{3}H]S produced comes directly from ECB-C(*S*-farnesyl)VI[^{3}H]S, the K_M of >30 μM for this reaction is significantly higher than the K_M of 1.1 μM for the production of VI[^{3}H]S from the farnesylated peptide. This suggests that the carboxypeptidase is not part of the pathway for the maturation of prenylated proteins. Nonprenylated peptides at concentrations of 10–100-fold higher than those of the prenylated substrates did not reduce the amount of tripeptide produced. The tripeptide-producing endoprotease is not inhibited by a number of well-known protease inhibitors. Studies with Percoll density gradient fractionation of rat liver membranes show that the endoprotease is localized mainly in the endoplasmic reticulum.

The posttranslational modification of eukaryotic peptides and proteins by the attachment of prenyl groups via a thioether linkage to cysteine residues has been reported (Clarke, 1992; Der & Cox, 1991; Gibbs, 1991; Glomset et al., 1990, 1991; Maltese, 1990; Rine & Kim, 1990; Sinensky & Lutz, 1992). So far, 15-carbon farnesyl and 20-carbon geranylgeranyl groups have been detected. For many proteins, the prenylation occurs on a cysteine that is part of the C-terminal amino acid sequence Cys-Ali-Ali-Xaa (Ali is usually, but not necessarily, an aliphatic amino acid and Xaa can be a variety of different amino acids). For these proteins it has been shown that prenylation occurs first, followed by selective proteolysis to remove the last three amino acids, and finally methylation of the newly exposed α-carboxyl group of the prenylated cysteine residue.

Protein farnesylation and geranylgeranylation are catalyzed by distinct prenyltransferases, and the type of prenyl group that is added to the protein is dictated primarily by the C-terminal amino acid (Xaa) (Casey et al., 1991; Finegold et al., 1991; Kohl et al., 1991; Moores et al., 1991; Reiss et al., 1991; Seabra et al., 1991; Yokoyama et al., 1991; Yoshida et al., 1991). The prenyl–cysteine α-carboxylmethyltransferase that utilizes *S*-adenosylmethionine as the methyl donor has been detected in the membrane fraction of yeast cells and mammalian tissue (Perez-Sala et al., 1991; Stephenson & Clarke, 1990). Genetic studies in yeast demonstrate that both farnesylated and geranylgeranylated cysteine residues are methylated by the same enzyme (Hrycyna et al., 1991; Volker et al., 1991).

Information about the enzyme(s) involved in the removal of the C-terminal three amino acids in prenylated Cys-Ali-Ali-Xaa-containing proteins is starting to emerge. Gutierrez and co-workers have provided direct evidence for the proteolysis event (Gutierrez et al., 1989). Expression of a mutant *ras* protein (p21$^{H\text{-}ras}$) in COS-1 cells that has a single radiolabeled tryptophan residue at its C-terminus results in the loss of the radiolabel during the maturation of the protein. More recently, Hancock and co-workers studied the *in vitro* translation of a gene for p21$^{K(B)\text{-}ras}$ in reticulocyte lysates and observed that the proteolysis and the subsequent methylation occurred if canine pancreatic microsomal membranes were added (Hancock et al., 1991). Proteolysis of synthetic farnesylated peptides has recently been detected in yeast and bovine liver membranes (Ashby et al., 1992; Ma & Rando, 1992). The major product formed is the tripeptide, Ali-Ali-Xaa, along with smaller amounts of dipeptide and single amino acid. Akopyan and co-workers observed that incubation of the prenylated peptide propionyl-GSPC(F)VLM [*S*-farnesylated and *S*-geranylgeranylated cysteine residues are designated as C(F) and C(GG), respectively] with mouse brain microsomes results in the release of methionine as the major product along with small amounts of leucine (Akopyan et al., 1992). Hrycyna and Clarke reported that yeast membranes are capable of cleaving the synthetic peptide *N*-acetyl-KSKTKC-(F)VIM to generate the substrate for the prenyl–cysteine α-carboxylmethyltransferase [*N*-acetyl-KSKTKC(F)] (Hrycyna & Clarke, 1992) but the identity of the C-terminal peptide product(s) was not determined.

† This work was supported by grants from the National Institutes of Health to M.H.G. (CA52874 and Research Career Development Award GM00562). M.H.G. is a Fellow of the Alfred P. Sloan Foundation (1991–1993).

* To whom correspondence should be addressed.

® Abstract published in *Advance ACS Abstracts,* August 15, 1993.

0006-2960/93/0432-9500$04.00/0

In the present study, synthetic prenylated peptides containing C-terminal radiolabeled amino acid residues have been prepared as substrates in order to detect protease activity in rat liver microsomes. The sequence of one peptide substrate corresponds to the C-terminus of the γ_6-subunit of bovine brain heterotrimeric G protein which has been shown to contain a C-terminal geranylgeranylated cysteine methyl ester (Yamane et al., 1990). The other peptide is patterned after the C-terminus of the farnesylated γ-subunit of transducin (Fukada et al., 1990; Lai et al., 1990). Results with these peptides are consistent with the earlier reports in that multiple proteolytic products are generated. A detailed kinetic analysis of the reaction products suggests that the Ali-Ali-Xaa-producing reaction is part of the maturation of prenylated proteins in mammalian tissue. Subcellular fractionation studies show that this enzyme, like the prenyl–cysteine methyltransferase (Stephenson & Clarke, 1992), localizes mainly in the endoplasmic reticulum.

MATERIALS AND METHODS

Materials. Enaliprilat and captopril were obtained as gifts from Merck Sharpe and Dohme and Bristol-Myers Squibb Research Labs, respectively. All other protease inhibitors were obtained from Sigma. The preparation, purification, and characterization of all peptides used in this study are provided as supplementary material. Preparation of rat liver microsomes and subcellular fractionation of rat liver homogenate are provided as supplementary material.

Assays for Proteolysis of Prenylated Peptides. Assays with ECB-NPFRQRRFFC(GG)AI[^{3}H]L[1] were carried out as follows. The standard reaction mixture contained 10 μL of buffer [100 mM glycine, 100 mM NaCl, and 16 μg/μL BSA (Sigma catalog no. A-7511), pH 9.5], 3 μL (45 μg of protein) of a suspension of washed rat liver microsomes, 1 μL of substrate stock ECB-NPFRQRRFFC(GG)AI[^{3}H]L in DMSO or DMF (final concentration in the assay of 2.2 μM, 0.2 μCi, 5 Ci/mmol, added last), and water to give a total volume of 20 μL. The reaction was incubated at 30 °C for 45 min (unless stated otherwise). To the reaction mixture was added 200 μL of 90% methanol containing 0.2 M acetic acid. After the insoluble material was pelleted with a microfuge, the pellet was extracted with 200 μL of the same solvent and the combined supernatants were dried down in a Speed-Vac. The residue was taken up in 50 μL of acetic acid/methanol containing 10 μg each of the peptides AIL and IL (as elution markers for the radiolabeled products). The mixture was injected onto the HPLC column (C_{18} reverse-phase column, 4.6 × 250 mm, Vydac 218TP, 10 μm), and the products were eluted under isocratic conditions (1 mL/min of 13.5% acetonitrile in water with 0.06% trifluoroacetic acid). The retention times for IL and AIL are 7.5 and 12.5 min, respectively. For measuring the amounts of peptide products, the eluants at 2.5–4.5 min (L), 6–8.5 min (IL), and 11–14 min (AIL) were collected, and an aliquot (0.7 mL) of each was mixed with 5 mL of scintillation cocktail and 6.3 μL of 1 M NaOH. The samples were submitted to scintillation counting. One microunit of activity is defined as the amount of enzyme in microsomes that produces 1 pmol of radioactive product/min with the standard assay conditions.

The assays with ECB-C(F)VI[^{3}H]S were carried out as follows. The standard reaction mixture contained 15 μL of buffer (100 mM glycine and 100 mM NaCl, pH 9.5), 1 μL of substrate stock in dimethylformamide (final concentration in the assay of 2.0–2.2 μM, 0.04 μCi, 1 Ci/mmol, unless stated otherwise, added last), other additives as noted, typically 3 μL (45 μg of protein) of a suspension of washed rat liver microsomes, and water to give a total volume of 25 μL. The reaction was incubated at 37 °C for 30 min (unless stated otherwise). The reaction was stopped by placing the reaction tube in boiling water for 3 min, and 125 μL of water and 10 μg of VIS were added. Precipitated protein was removed in a microfuge and 145 μL of the supernatant was injected onto the HPLC column, and the products were eluted with an isocratic solvent mixture (2.5% acetonitrile in water with 0.06% trifluoroacetic acid) with a flow rate of 1 mL/min. Serine eluted in the solvent front and the retention times for IS and VIS are 5.5 and 13.5 min, respectively. For quantifying the amounts of peptide products, the eluants at 2.5–4.0 min (S), 4.5–6.5 min (IS), and 12–15 min (VIS) were collected, and an aliquot (0.5 mL) of each was mixed with 3 mL of scintillation cocktail. The samples were submitted to scintillation counting. Some assays were carried out at pH 7.6 in an identical manner except that 100 mM glycine was replaced by 100 mM HEPES.

For TLC analysis, the peak fractions from the HPLC column were dried in a Speed-Vac, and the residue was dissolved in a small volume of methanol (for AIL) or water (for VIS) and spotted onto a TLC plate (Merck silica gel 60, without fluorescent indicator, 0.2 mm, 20 × 20 cm). The plates were developed with chloroform/methanol/32% aqueous acetic acid (5:3:1 v/v/v). Fluorography of TLC plates was carried out by spraying the dry plate with EN^{3}HANCE (NEN), wrapping the plate with Saran Wrap, and placing the plate in a film cassette with an intensifying screen (Kodak X-Omatic) and X-ray film (Kodak X-Omat AR) at −80 °C for 48 h.

Studies with Protease Inhibitors. Rat liver microsomal protein (45 μg) was preincubated in standard assay buffer (10 μL) containing various protease inhibitors and water (to bring the total volume to 20 μL) for 20 min at ambient temperature. The reaction was initiated by addition of substrate and analyzed as described for the standard assay.

RESULTS

Proteolysis of ECB-NPFRQRRFFC(GG)AI[^{3}H]L by Rat Liver Microsomes. In order to identify a protease activity specific for prenylated proteins, a geranylgeranylated peptide patterned after the C-terminal 13 amino acids of the γ_6-subunit was synthesized. In addition, a radiolabeled leucine was placed at the C-terminus of the peptide so that proteolytic product(s) could be detected. This latter step is greatly facilitated by eliminating all of the amino acid side chains that can react with the peptide coupling reagent. Thus, the two lysine residues were changed to arginine residues and the glutamate was changed to glutamine. The peptide ECB-NPFRQRRFFCAI was prepared by machine synthesis and converted to the final product, ECB-NPFRQRRFFC(GG)AI[^{3}H]L, using solution chemical reactions as described in Materials and Methods. The ECB group was added to the peptide for the eventual use of solid-phase-bound avidin in a rapid protease assay.

Incubation of ECB-NPFRQRRFFC(GG)AI[^{3}H]L (2.2 μM) with rat liver microsomes in buffer (50 mM glycine, 50

[1] Abbreviations: BSA, bovine serum albumin; CAPS, 3-(cyclohexylamino)-1-propanesulfonic acid; DTT, dithiothreitol; ECB, extended-chain biotinyl group [biotin-CONH-$(CH_2)_5$-CO-]; EDTA, ethylenediaminetetraacetic acid; EGTA, ethylene glycol bis(β-aminoethyl ether)-*N,N,N',N'*-tetraacetic acid; HEPES, *N*-(2-hydroxyethyl)piperazine-*N'*-ethanesulfonic acid; [^{3}H]L, [4,5-^{3}H]-L-leucine; PMSF, phenylmethanesulfonyl fluoride; [^{3}H]S, [3-^{3}H]-L-serine; TLCK, *N*-tosyl-L-lysine chloromethyl ketone; TPCK, *N*-tosyl-L-phenylalanine chloromethyl ketone.

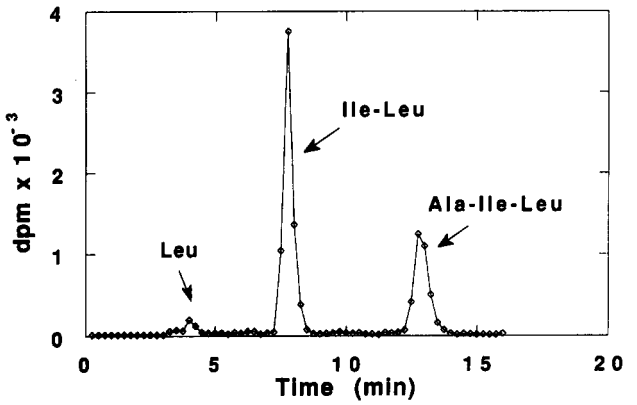

FIGURE 1: Reverse-phase HPLC analysis of radioactive products derived from the proteolysis of ECB-NPFRQRRFFC(GG)AI[^{3}H]L. The assay was conducted using the standard reaction protocol with 45 μg of microsomal protein.

mM NaCl, and 8 μg/μL BSA, pH 9.5) leads to three radioactive products that are separable by HPLC (Figure 1). The small peak of radiolabeled material that elutes near the solvent front was identified as [^{3}H]L, on the basis of comigration with an authentic standard on a silica gel TLC plate. The amount of [^{3}H]L detected was <5% of the total amount of I[^{3}H]L and AI[^{3}H]L formed. The other two peaks were identified by coelution with authentic standards on HPLC to be I[^{3}H]L and AI[^{3}H]L (retention times 7.5 and 12.5 min, respectively) and by comigration on TLC (not shown). When the HPLC column was further developed for a prolonged time with a gradient ending in 100% acetonitrile/0.06% trifluoroacetic acid after the elution of the short peptides, only the unreacted substrate ECB-NPFRQRRFFC(GG)AI[^{3}H]L was detected. This establishes that there is no proteolytic cleavage on the N-terminal side of the C(GG) residue. The specific activities for the protease activities in rat liver microsomes measured with standard assay are 0.38 microunit/mg for I[^{3}H]L and 0.13 microunit/mg for AI[^{3}H]L. The specific activities for the production of I[^{3}H]L and AI[^{3}H]L when ECB-NPFRQRRFFC(GG)AI[^{3}H]L was incubated with rat liver cytosol are only 3% and 2%, respectively, of those measured with membranes.

The I[^{3}H]L-producing activity is maximal in the range pH 7–8, and the activity decreases both below and above this pH range. The AI[^{3}H]L-producing activity increases steadily when the pH is increased from 5 to 9.5. At pH 7, the I[^{3}H]L to AI[^{3}H]L ratio is 10, whereas at pH 9.5, the ratio drops to approximately 2.5. These results are consistent with the idea that I[^{3}H]L and AI[^{3}H]L are produced by distinct enzymes.

The dependencies of the initial reaction velocities for the production of AI[^{3}H]L and I[^{3}H]L on the concentration of the ECB-NPFRQRRFFC(GG)AI[^{3}H]L substrate display hyperbolic patterns (not shown). From double-reciprocal plots, the K_M and V_{max} values for I[^{3}H]L production are found to be 1.1 μM and 0.3 pmol min^{-1} mg^{-1}, respectively, and those for the AI[^{3}H]L production are 2.5 μM and 0.4 pmol min^{-1} mg^{-1}, respectively.

Specificity of the Proteases for Prenylated versus Nonprenylated Peptides. The inhibition of the proteolysis reactions by nonprenylated peptides was studied in order to determine if the proteases involved in the formation of AI[^{3}H]L and I[^{3}H]L are specific for prenylated peptides. As shown in Figure 2A, the nonprenylated peptide in which the geranylgeranyl cysteine residue is replaced by alanine (ECB-NPFRQRRFFAAIL) is a more potent inhibitor of I[^{3}H]L production than of AI[^{3}H]L production from ECB-NPFRQRRFFC(GG)AI[^{3}H]L. For example, in the presence of 20 μM nonprenylated peptide (10-fold excess over substrate), the formation of I[^{3}H]L is inhibited by 40%, whereas the production of AI[^{3}H]L is not affected. With higher concentrations of the nonprenylated peptide, both activities are partially inhibited. The rise in the level of AI[^{3}H]L seen with 10 μM nonprenylated peptide is due to the inhibition of the secondary proteolysis of the tripeptide as discussed below.

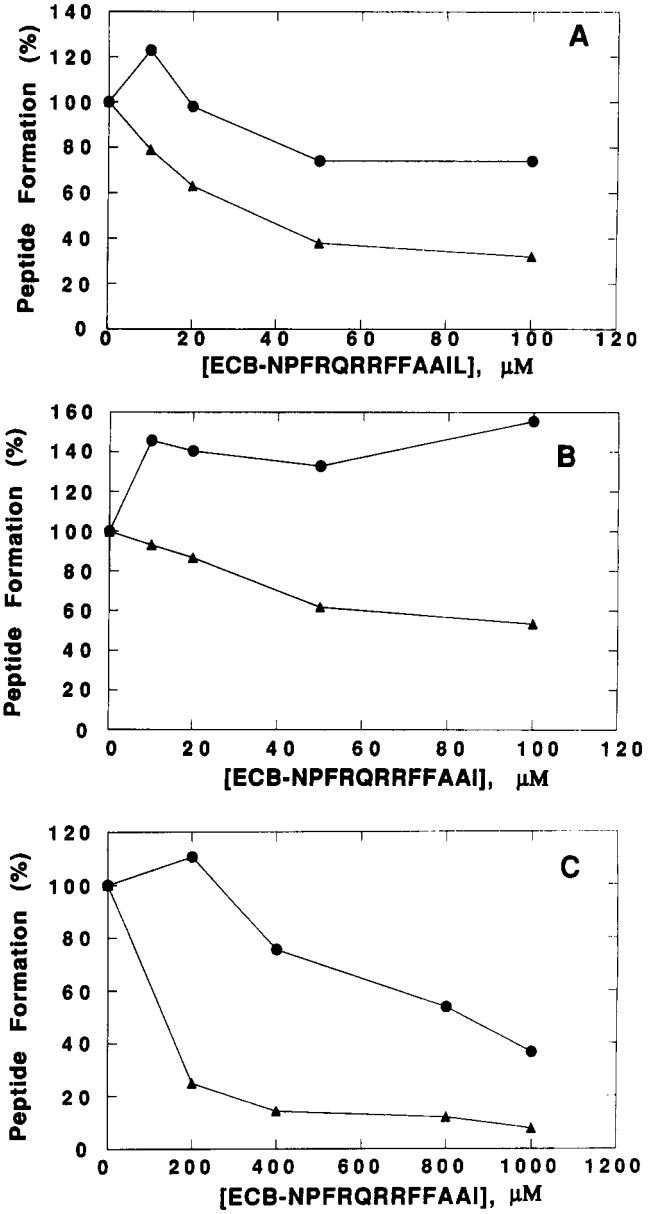

FIGURE 2: (A) Inhibition of short-peptide production from ECB-NPFRQRRFFC(GG)AI[^{3}H]L by the nonprenylated full-length peptide ECB-NPFRQRRFFAAIL. The percentage of I[^{3}H]L (triangles) and the percentage of AI[^{3}H]L (circles) produced using the standard protocol in the presence of the indicated concentration of the nonprenylated peptide is compared to that produced in the absence of this peptide. The nonprenylated peptide was added from a stock solution in 50% aqueous methanol so that the amount of methanol in the assay was 5%. (B and C) Inhibition of I[^{3}H]L (triangles) and AI[^{3}H]L (circles) production from ECB-NPFRQ-RRFFC(GG)AI[^{3}H]L by the nonprenylated peptide ECB-NP-FRQRRFFAAI. Conditions were the same as in panel A except that the peptide inhibitor was used at concentrations of 0–100 μM (B) or up to 1000 μM (C). The peptide inhibitor was added from a stock solution in water.

The radiolabeled nonprenylated peptide ECB-NPFRQR-RFFAAI[^{3}H]L was also prepared and tested as a substrate.

Product analysis by HPLC using the conditions shown in Figure 1 reveals peaks of radioactivity at the retention times corresponding to [^{3}H]L, I[^{3}H]L, and AI[^{3}H]L. TLC analysis of the radioactive material eluting from the HPLC column confirms that the first two HPLC peaks are [^{3}H]L and I[^{3}H]L, respectively. TLC analysis of the HPLC peak at the position of AI[^{3}H]L reveals two spots, one at the position of AI[^{3}H]L (R_f 0.52, about 10% of the material) and the remaining 90% of the radioactivity runs just behind (R_f 0.49) AI[^{3}H]L and is most likely a longer peptide. The ratio of specific activities for the three peptide products derived from the nonprenylated peptide ECB-NPFRQRRFFAAI[^{3}H]L to those measured with the prenylated peptide ECB-NPFRQRRFFC(GG)AI-[^{3}H]L are 37 for [^{3}H]L, 20 for I[^{3}H]L, and 0.7 for AI[^{3}H]L.

The truncated and nonprenylated peptide ECB-NPFRQR-RFFAAI was also tested as an inhibitor of I[^{3}H]L and AI-[^{3}H]L formation from ECB-NPFRQRRFFC(GG)AI[^{3}H]L. The results shown in Figure 2B,C indicate that with concentrations of nonprenylated peptide in the range 0–100 μM, the formation of I[^{3}H]L is inhibited by about 50%, whereas the production of AI[^{3}H]L is increased. In the presence of 200 μM ECB-NPFRQRRFFAAI, the formation of I[^{3}H]L is inhibited by 80%, whereas the formation of AI[^{3}H]L is not inhibited. Significant inhibition of AI[^{3}H]L production occurs only when the concentration of the nonprenylated peptide exceeds 200 μM.

Source of I[^{3}H]L and AI[^{3}H]L. Experiments were carried out in order to determine if both I[^{3}H]L and AI[^{3}H]L are produced directly from the prenylated peptide or whether I[^{3}H]L is generated from proteolysis of AI[^{3}H]L. The addition of a 140-fold excess (0.3 mM) of unlabeled AIL over ECB-NPFRQRRFFC(GG)AI[^{3}H]L does not reduce the amount of I[^{3}H]L formed. There are two reasonable explanations for this result. The first is that I[^{3}H]L comes directly from the prenylated peptide and AIL does not inhibit this process. The second is that a microsomal protease acts on AI[^{3}H]L to form I[^{3}H]L + A and that the K_M for AI[^{3}H]L is >0.3 mM. Thus, the 140-fold increase in the concentration of AIL leads to an increase in the rate of cleavage of the tripeptide by the same factor (first-order kinetics when substrate is below its K_M). However, the 140-fold drop in specific radioactivity of AI[^{3}H]L leads to no change in the amount of I[^{3}H]L formed. Thus, additional experiments are required to determine the source of the I[^{3}H]L.

The rat liver microsomes are capable of cleaving AI[^{3}H]L to give I[^{3}H]L as the major product (90%) and [^{3}H]L as the minor product (10%). Incubation of 0.22 μM AI[^{3}H]L with microsomes under the same conditions used in the standard assay with ECB-NPFRQRRFFC(GG)AI[^{3}H]L leads to a first-order loss of AI[^{3}H]L with a rate constant of 0.15 min^{-1} (half-time of 4.6 min). The time course of formation of AI-[^{3}H]L and I[^{3}H]L from ECB-NPFRQRRFFC(GG)AI[^{3}H]L was studied and the results are presented in Figure 3A. The amount of I[^{3}H]L rises over a 2-h period, whereas the level of AI[^{3}H]L production reaches a plateau level during this time period (studies described below show that the tripeptide-producing enzyme is stable for the duration of this time course). This behavior is consistent with the notion that I[^{3}H]L is generated from AI[^{3}H]L and thus AI[^{3}H]L reaches a steady-state level while I[^{3}H]L continues to increase.

The data in Figure 2 also support the idea that much of the I[^{3}H]L comes from AI[^{3}H]L. The nonprenylated peptide ECB-NPFRQRRFFAAI at concentrations below 200 μM causes a decrease in the amount of I[^{3}H]L with a concomitant increase in the amount of AI[^{3}H]L. The increase in the level of AI[^{3}H]L in the presence of 20 μM nonprenylated peptide (1800 dpm) is similar to the amount of decrease in the level of I[^{3}H]L (2400 dpm), which strongly suggests that AI[^{3}H]L is the source of I[^{3}H]L. Similarly, an increase in the amount of AI[^{3}H]L is seen with a low concentration of ECB-NPFRQRRFFAAIL (10 μM).

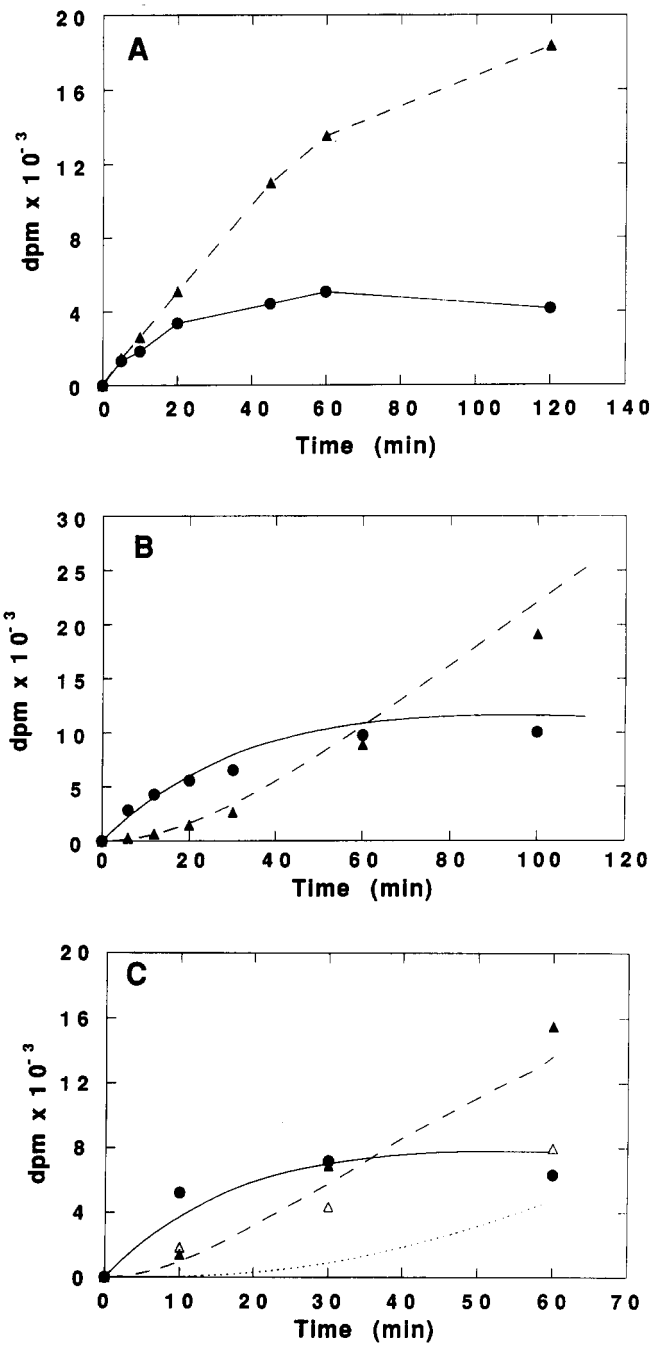

FIGURE 3: Reaction progress curves for proteolysis of prenylated peptides. (A) AI[^{3}H]L (circles) and I[^{3}H]L (triangles) production from ECB-NPFRQRRFFC(GG)AI[^{3}H]L was determined using the standard assay conditions except that the temperature was 37 °C. (B) VI[^{3}H]S (circles) and I[^{3}H]S (triangles) production from ECB-C(F)VI[^{3}H]S was determined using the assay conditions at pH 9.5. The computer-simulated curves and rate constants are follows: solid line, VI[^{3}H]S, pseudo-first-order rate constant 0.0033 min^{-1}; dashed line, I[^{3}H]S, first-order rate constant 0.025 min^{-1}. (C) VI[^{3}H]S (circles), I[^{3}H]S (filled triangles), and [^{3}H]S (open triangles) production from ECB-C(F)VI]^{3}H]S was determined using the assay conditions at pH 7.6. The computer-simulated curves and rate constants are as follows: solid line, VI[^{3}H]S, pseudo-first-order rate constant 0.0050 min^{-1}; dashed line, I[^{3}H]S, first-order rate constant 0.05 min^{-1}; dotted line, [^{3}H]S, first-order rate constant 0.0132 min^{-1}.

Table I: Distribution of Protease Activities between Microsomal, Mitochondrial, and Nuclear Fractions[a]

subcellular fraction	I[^{3}H]L-producing activity	AI[^{3}H]L-producing activity	citrate synthase activity	glucose-6-phosphatase activity
microsomes	66 (81)	59 (80)	0 (0)	71 (78)
mitochondria	14 (15)	10 (12)	91 (98)	22 (20)
nuclei	20 (4)	31 (8)	9 (2)	7 (2)

[a] The numbers are the percent of the specific activity, and the numbers in parentheses are the percent of the total activity for each enzyme in the indicated fractions.

Consistent with the model in which I[^{3}H]L comes from AI[^{3}H]L is the fact that the K_M values for the formation of AI[^{3}H]L and I[^{3}H]L based on the concentration of ECB-NPFRQRRFFC(GG)AI[^{3}H]L are similar (2.5 and 1.1 μM, respectively). If I[^{3}H]L comes from AI[^{3}H]L, the K_M for the formation of the dipeptide is necessarily similar to the K_M for the formation of the tripeptide. This is because the rate of AI[^{3}H]L formation will be constant as the concentration of ECB-NPFRQRRFFC(GG)AI[^{3}H]L is increased in the region above its K_M and thus the rate of I[^{3}H]L production will also be constant in this region if it comes from AI[^{3}H]L.

Inhibition Studies with Known Protease Inhibitors. The rat liver membranes were preincubated with a number of different known protease inhibitors in order to determine whether these compounds reduce the production of I[^{3}H]L and AI[^{3}H]L from ECB-NPFRQRRFFC(GG)AI[^{3}H]L. The following compounds produce less than 20% inhibition of the formation of I[^{3}H]L and AI[^{3}H]L: aprotinin (0.8 mg/mL), benzamidine (1 mM), captopril (2 μM), diisopropyl fluorophosphate (DFP) (4 mM), DTT (1 mM), EDTA (1 mM), EGTA (1 mM), elastinal (0.1 mM), Enaprilat (2 μM), *trans*-epoxysuccinyl-L-leucylamido-(4-guanidino)butane (E-64) (1 mM), *N*-ethylmaleimide (1 mM), *o*-phenanthroline (0.1 mM), PMSF (4 mM), soybean trypsin inhibitor (0.8 mg/mL), TLCK (0.1 mM), and TPCK (0.1 mM). 4-(Hydroxymercuri)-benzoate (0.5 mM) inhibits the formation of I[^{3}H]L and AI-[^{3}H]L by 96% and 90%, respectively. Pepstatin (0.1 mM) inhibits the formation of I[^{3}H]L by 60% but does not inhibit the formation of AI[^{3}H]L. Leupeptin (0.1 mM) inhibits I[^{3}H]L formation by 53% and AI[^{3}H]L formation by 40%. Zinc chloride (0.25 mM) does not inhibit I[^{3}H]L formation but AI[^{3}H]L formation is inhibited by 74%. Preincubation of the membranes with ebelcatone B (0–100 μm) for 10 min inhibits the formation of I[^{3}H]S from ECB-C(F)VI[^{3}H]S (see below) by approximately 30% at the highest concentration tested, and no inhibition of VI[^{3}H]S was observed. The different effect of protease inhibitors suggests that dipeptide and tripeptide are products of distinct enzymes.

Rat liver microsomes were prepared with homogenation buffer containing several protease inhibitors that do not strongly inhibit the production of AI[^{3}H]L (see Materials and Methods). For AI[^{3}H]L production, the inclusion of protease inhibitors results in a slight (1.5-fold) increase in the specific activity, whereas the specific activity for I[^{3}H]L production drops by 1.7-fold.

Subcellular Fractionation Studies. As shown in Table I, most of the I[^{3}H]L and AI[^{3}H]L-producing activities are associated with rat liver microsomes. The levels of protease activities correlate with the level of the microsomal marker (glucose-6-phosphatase) rather than with the mitochondrial marker (citrate synthase), and relatively small amounts of proteases were detected in the nuclear pellet. The postnuclear

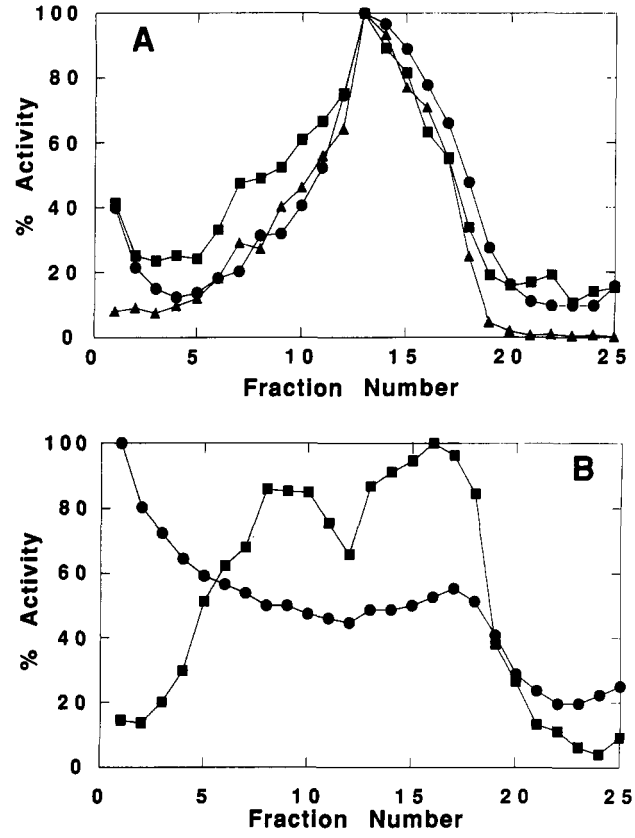

FIGURE 4: Percoll density gradient centrifugation of rat liver membranes (fraction 1 is from bottom of the tube). (A) Analysis of Percoll gradient fractions for the endoplasmic reticulum marker (glucose-6-phosphatase, circles), the I[^{3}H]L-producing protease (triangles), and the AI[^{3}H]L-producing protease (squares). (B) Same as in (A) but the assays were for the plasma membrane marker (5′-nucleotidase, circles) and the golgi marker (galactosyltransferase, squares).

fraction was submitted to Percoll density gradient ultracentrifugation. The results are summarized in Figure 4. Both the I[^{3}H]L- and AI[^{3}H]L-producing activities localize with the endoplasmic reticulum enzyme marker (glucose-6-phosphatase) and are well separated from the bulk of the plasma membrane and golgi enzyme markers (5′-nucleotidase and galactosyltransferase, respectively).

Proteolysis of ECB-C(F)VI[^{3}H]S and the Source of the Products. The farnesylated substrate ECB-C(F)VI[^{3}H]S is patterned after the C-terminal portion of the γ-subunit of transducin (Fukada et al., 1990; Lai et al., 1990). Incubation of ECB-C(F)VI[^{3}H]S with rat liver microsomes in buffer at pH 7.6 leads to three radioactive products which were identified by HPLC and TLC to be [^{3}H]S, I[^{3}H]S, and VI[^{3}H]S in the ratio of 0.6:1.2:1.0. Incubation at pH 9.5 leads to the same radioactive products but in a ratio of 0.05:0.4:1. Under this condition, the specific activity for the production of VI[^{3}H]S is 2.7 microunits/mg, and this value is 20-fold greater than that for the production of AI[^{3}H]L from ECB-NPFRQR-RFFC(GG)AI[^{3}H]L under the same assay conditions.

Experiments were carried out to determine the source of I[^{3}H]S and VI[^{3}H]S. The reaction progress for the proteolysis of ECB-C(F)VI[^{3}H]S at pH 9.5 is shown in Figure 3B. The production of VI[^{3}H]S reaches a steady-state level after about 60 min. The formation of I[^{3}H]S initially lags behind VI-[^{3}H]S production and eventually it becomes the major radiolabeled peptide product. These results suggest that I[^{3}H]S is generated from VI[^{3}H]S. The amount of [^{3}H]S is less than 5% of the sum of I[^{3}H]S and VI[^{3}H]S at all time

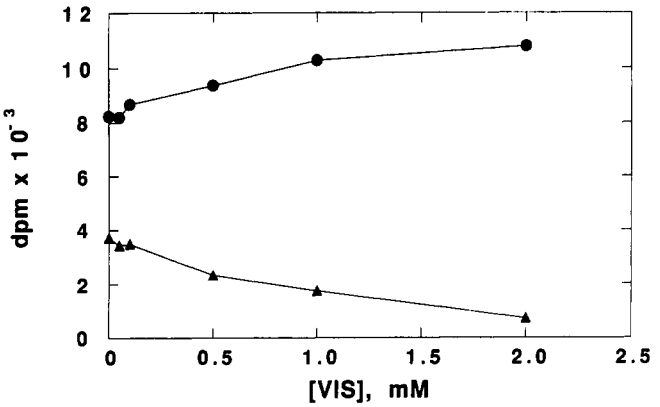

FIGURE 5: Effect of VIS on the production of VI[^{3}H]S (circles) and I[^{3}H]S (triangles) from ECB-C(F)VI[^{3}H]S. The assay protocol at pH 9.5 was used in the presence of the indicated concentration of the unlabeled peptide VIS. THe peptide was incubated with rat liver microsomes for 10 min at room temperature before the substrate was added.

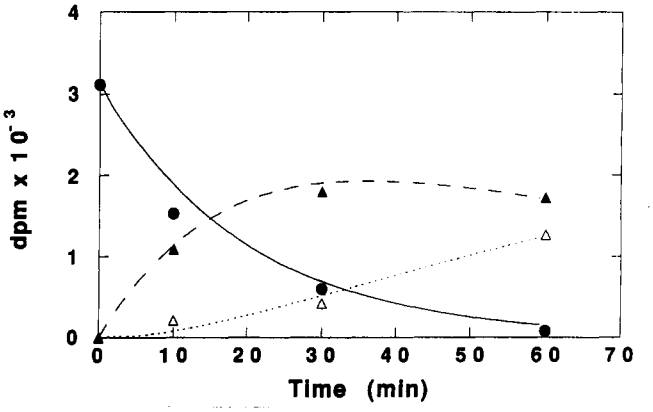

FIGURE 6: Proteolysis of VI[^{3}H]S by rat liver microsomes at pH 7.6. The loss of VI[^{3}H]S is shown by the circles and the simulated curve (first-order rate constant 0.05 min^{-1}) is shown by the solid line. The formation of I[^{3}H]S is shown by the triangles and the simulated curve is shown by the dashed line. The formation of [^{3}H]S is shown by the open triangles and the simulated curve (first-order rate constant 0.0132 min^{-1}) is shown by the dotted line.

points. Incubation of VI[^{3}H]S with the rat liver microsomes under identical conditions leads to a first-order loss of the tripeptide and a concomitant formation of I[^{3}H]S as the major product (not shown). The amount of [^{3}H]S was <5% of I[^{3}H]S at all time points. Furthermore, when I[^{3}H]S was incubated with the microsomes, only about 20% of it was converted to [^{3}H]S after 20 h. The rate constant for the proteolysis of VI[^{3}H]S to give I[^{3}H]S is 0.025 min^{-1} (half-time 28 min). As shown in Figure 3B, the kinetics for the formation of I[^{3}H]S and VI[^{3}H]S are well simulated using the observed initial rate constant for the formation of the tripeptide from the full-length substrate and the observed rate constant for the secondary proteolysis of the tripeptide to give the dipeptide.

The dependency of the initial velocity for the formation of VI[^{3}H]S on the concentration of ECB-C(F)VI[^{3}H]S displays hyperbolic kinetics and the values of K_M and V_{max} of 6.7 μM and 8 pmol min^{-1} mg^{-1}, respectively, were obtained from the double-reciprocal plots (not shown). The K_M for the formation of I[^{3}H]S from the farnesylated peptide is 4.8 μM. The similarity in the K_M values for these two enzymatic processes also suggests that I[^{3}H]S comes from VI[^{3}H]S. In contrast, the rate of [^{3}H]S production shows a linear dependence on the concentration of the peptide substrate up to 30 μM and thus the K_M for this reaction must be greater than 30 μM.

The results shown in Figure 5 are also supportive of a two-enzyme proteolysis sequence. It can be seen that the production of I[^{3}H]S from ECB-C(F)VI[^{3}H]S is inhibited by inclusion of a large concentration of unlabeled VIS in the incubation mixture, whereas the production of VI[^{3}H]S increases. At all concentrations of VIS tested, the sum of the dpm from I[^{3}H]S and VI[^{3}H]S remains constant. This result implies that essentially all of the I[^{3}H]S comes from proteolysis of VI[^{3}H]S. If I[^{3}H]S and VI[^{3}H]S come from the action of distinct enzymes, both acting on ECB-C(F)VI[^{3}H]S, no increase in the amount of VI[^{3}H]S formed would be observed. If the dipeptide and tripeptide are produced by a single enzyme acting at different sites in ECB-C(F)VI[^{3}H]S, a decrease in the production of both products would be observed. The results in Figure 5 also establish that the VI[^{3}H]S-producing enzyme is not inhibited by millimolar concentrations of one of its products.

The proteolysis of ECB-C(F)VI[^{3}H]S was also studied at pH 7.6 and the reaction progress is given in Figure 3C. The major product at early times is VI[^{3}H]S, but I[^{3}H]S is the major product at later times. In addition, [^{3}H]S formation is significantly higher at pH 7.6 (Figure 3C) than at pH 9.5. In order to study the source of these products, the proteolysis of VI[^{3}H]S by the microsomes at pH 7.6 was measured. The data in Figure 6 show that VI[^{3}H]S is converted to both I[^{3}H]S and [^{3}H]S. It is apparent from the early time points that the VI[^{3}H]S is hydrolyzed to give mainly I[^{3}H]S, suggesting that [^{3}H]S comes from proteolysis of I[^{3}H]S. This was found to be the case. Incubation of I[^{3}H]S with microsomes leads to a first-order production of [^{3}H]S with a rate constant of 0.0132 min^{-1} (half-time 52 min). The observed kinetics shown in Figure 6 are well simulated by a consecutive first-order sequence using a first-order rate constant for the conversion of VI[^{3}H]S to I[^{3}H]S of 0.05 min^{-1} (half-time 13.9 min) (derived from the observed initial rate of I[^{3}H]S formation) and the observed rate constant for conversion of I[^{3}H]S to [^{3}H]S of 0.0132 min^{-1}.

As shown in Figure 3C, kinetic simulation suggests that I[^{3}H]S comes from VI[^{3}H]S since the data are well described by the observed initial rate of VI[^{3}H]S production from ECB-C(F)VI[^{3}H]S and the observed rate of proteolysis of the tripeptide to give the dipeptide. However, this is not the case for the kinetics of [^{3}H]S formation. As shown in Figure 3C, the initial rate of [^{3}H]S production is faster than that given by the conversion of I[^{3}H]S to [^{3}H]S (using the measured rate constant of 0.0132 min^{-1}, see above). This suggests that at least some of the [^{3}H]S comes from direct proteolysis of ECB-C(F)VI[^{3}H]S. The dependencies of the rates of formation of VI[^{3}H]S and I[^{3}H]S on the concentration of ECB-C(F)VI[^{3}H]S display hyperbolic patterns (not shown). From double-reciprocal plots, the V_{max} for VI[^{3}H]S formation is 7 pmol min^{-1} mg^{-1}. The K_M values for VI[^{3}H]S and I[^{3}H]S formation are similar, 1.1 and 1.4 μM, respectively, which supports the notion that the dipeptide comes from the tripeptide. In marked contrast, the formation of [^{3}H]S from ECB-C(F)VI[^{3}H]S shows a linear dependence on the concentration of the prenylated peptide up to the maximal concentration tested (30 μM). This result shows that the K_M for this reaction is significantly above 30 μM, as is the case at pH 9.5, and it establishes that the bulk of the [^{3}H]S is due to direct proteolysis of ECB-C(F)VI[^{3}H]S rather than secondary proteolysis.

Inhibition Studies with ECB-C(F)VI[^{3}H]S. The proteolysis of ECB-C(F)VI[^{3}H]S (2 μM) was studied at pH 9.5 in the presence of various amounts of the nonfarnesylated peptide

ECB-CVIS. No inhibition of VI[^{3}H]S production was observed when ECB-CVIS was included in the incubations at concentrations of 0–800 μM. In the presence of 800 μM ECB-CVIS, only 20% inhibition of I[^{3}H]S from ECB-C(F)VI-[^{3}H]S was observed. The truncated and prenylated peptide ECB-C(F)VI inhibited the production of both VI[^{3}H]S and I[^{3}H]S from ECB-C(F)VI[^{3}H]S by 50% when present at a concentration of 20 μM.

DISCUSSION

In the protein prenylation pathway, the three amino acids on the C-terminal side of the prenylated cysteine residue are removed. This proteolytic event could occur by different routes in which single amino acids, dipeptides, or a tripeptide are produced. Results described herein indicate that a single endoproteolytic event to produce an intact tripeptide (Ali-Ali-Xaa) is the major process for the maturation of prenylated peptides and proteins in rat liver microsomes. Incubation of the prenylated peptide ECB-NPFRQRRFFC(GG)AI[^{3}H]L with rat liver microsomes, but not cytosol, gives rise to mainly AI[^{3}H]L and I[^{3}H]L. Several independent experiments show that most of the I[^{3}H]L is formed from AI[^{3}H]L by secondary proteolysis.

The tripeptide-producing enzyme is unique in displaying specificity for the prenylated versus the nonprenylated substrate, although this specificity is not absolute. For example, the presence of the nonprenylated peptide ECB-NPFRQR-RFFAAIL in 10-fold excess over the prenylated peptide substrate ECB-NPFRQRRFFC(GG)AI[^{3}H]L does not reduce the amount of AI[^{3}H]L formed, but higher concentrations do produce some inhibition (Figure 2A). In addition, concentrations of ECB-NPFRQRRFFAAI of more than 100-fold above the concentration of the prenylated peptide are needed to cause a decrease in the production of AI[^{3}H]L (Figure 2B,C). In contrast, the nonprenylated peptide inhibited I[^{3}H]L production at all concentrations tested. Ma and Rando have shown that in the case of proteolysis of *N*-acetyl-C(F)VI[^{3}H]S by bovine liver microsomes, the presence of a 5-fold excess of the nonprenylated peptide (*N*-acetyl-CVIS) does not lead to a reduction in the amount of VI[^{3}H]S formed (Ma & Rando, 1992). With yeast membranes, the proteolysis of *N*-dansyl-WDPAC(F)VIA to give *N*-dansyl-WDPAC(F) is inhibited by 40% in the presence of a 4-fold excess of nonprenylated a-factor (Ashby et al., 1992).

A number of well-known inhibitors of serine, cysteine, and aspartic acid proteases and zinc metalloproteases did not significantly inhibit the production of AI[^{3}H]L. Ashby et al. (1992) found that the prenylated peptide protease in yeast membranes is not inhibited by PMSF or *o*-phenanthroline but is inhibited by 100 μM Zn^{2+}. The same results are obtained with the rat liver enzyme. Ebelactone B, at a concentration of around 50 μM, has recently been reported to inhibit *S*-farnesyl-cysteine methyl esterase activity present in bovine rod outer segment membranes (Tan & Rando, 1992). The fact that this compound at concentrations of 0–100 μM does not inhibit the formation of VI[^{3}H]S from ECB-C(F)VI[^{3}H]S strongly suggests that the protease and the methyl esterase are distinct enzymes.

Subcellular fractionation studies indicate that most of the AI[^{3}H]L-producing enzyme is associated with endoplasmic reticulum membranes and is possibly colocalized with the prenylated cysteine α-carboxylmethyltransferase (Hrycyna & Clarke, 1992). Thus, in the posttranslational modification of Cys-Ali-Ali-Xaa-containing proteins, only the prenylation reaction occurs in the aqueous phase. An interesting question that remains is how specific prenylated proteins become targeted to specific cellular membranes.

The major products derived from the farnesylated peptide ECB-C(F)VI[^{3}H]S at pH 9.5 are VI[^{3}H]S and I[^{3}H]S. Again, it is shown that the dipeptide comes from the proteolysis of the tripeptide. These results are similar to those reported by Ma and Rando (1992) for the proteolysis of *N*-acetyl-C(F)-VI[^{3}H]S by bovine liver microsomes, except that the proteolysis of the tripeptide is apparently more rapid with the rat liver microsomes. On the other hand, the specific activities measured for the production of C-terminal tripeptides from farnesylated substrates are similar with the rat liver and bovine liver microsomes.

At pH 7.6, but not at pH 9.5, [^{3}H]S is produced by direct proteolysis of ECB-C(F)VI[^{3}H]S. This type of carboxypeptidase activity was not seen in the studies with bovine liver microsomes (Ma & Rando, 1992), but Akopyan et al. (1992) reported that incubation of the prenylated peptide propionyl-GSOC(F)VLM with mouse brain microsomes results in the release of methionine as the major product along with small amounts of leucine. Interestingly, the pH optimum for this mouse brain enzyme is around 7.2, which is similar to our findings for the production of [^{3}H]S from ECB-C(F)VI[^{3}H]S. The K_M value of 73 μM is reported for the mouse brain enzyme-catalyzed production of methionine from propionyl-GSPC-(F)VLM (Akopyan et al., 1992). In the present studies, it is shown that the K_M for the production of [^{3}H]S from ECB-C(F)VI[^{3}H]S is significantly above 30 μM. The K_M for this enzymatic reaction is more than 30-fold above the K_M of 1.1 μM for the production of VI[^{3}H]S from the same substrate. This result together with the fact that a relatively large amount of carboxypeptidase activity is detected in these membranes with the nonprenylated substrate ECB-NPFRQRRFFAAI-[^{3}H]L suggests that this carboxypeptidase reaction is not part of the prenylated protein maturation process.

Akopyran and co-workers reported a K_M of 600 μM for the production of methionine from the nonfarnesylated peptide propionyl-GSPCVLM, which is about 10-fold higher than the K_M for the production of methionine from the farnesylated peptide. This result should not be interpreted as evidence that the production of methionine requires a protease that interacts directly with the prenyl group. In these reactions, the prenyl group may simply allow the peptide to bind to the membrane where it can encounter the membrane-bound protease(s). In the present study, it was found that the inclusion of the nonprenylated peptide ECB-CVIS at concentrations up to 400-fold higher than the concentration of ECB-C(F)VI[^{3}H]S did not reduce the amount of VI[^{3}H]S or I[^{3}H]S formed. This result is likely due to the fact that ECB-CVIS is expected to be mainly in the aqueous phase. The inhibition of the production of both AI[^{3}H]L and I[^{3}H]L from the prenylated peptide ECB-NPFRQRRFFC(GG)AI-[^{3}H]L by the nonprenylated peptide ECB-NPFRQRRF-FAAIL (Figure 2A) may be due to the fact that this peptide is highly cationic and is likely to bind to the negative surface of membranes via electrostatic interactions, where it can interact with the membrane-found proteases. Studies are underway to determine if the prenyl group of the substrate directly interacts with the membrane-bound tripeptide-producing endoprotease.

ACKNOWLEDGMENT

We are grateful to Patrick Chou and Henry Zebroski for the synthesis of peptides and to Wendy E. Thomas for technical assistance. Some of the peptides were synthesized at the

University of Washington Molecular Pharmacology Facility. The mass spectrometry was carried out at the University of Washington (NIH 02262).

SUPPLEMENTARY MATERIAL AVAILABLE

A description of the preparation, purification, and characterization of all peptides used in this study and of the preparation of rat liver microsomes and subcellular fractionation of rat liver homogenate (9 pages). Ordering information is given on any current masthead page.

REFERENCES

Akopyan, T. N., Couedel, Y., Beaumont, A., Fournie-Zaluski, M.-C., & Roques, B. P. (1992) *Biochem. Biophys. Res. Commun. 187*, 1336–1342.

Ashby, M. N., King, D. S., & Rine, J. (1992) *Proc. Natl. Acad. Sci. U.S.A. 89*, 4613–4617.

Casey, P. J., thissen, J. A., & Moomaw, J. F. (1991) *Proc. Natl. Acad. Sci. U.S.A. 88*, 8631–8635.

Clarke, S. (1992) *Annu. Rev. Biochem. 61*, 355–386.

Der, C. J., & Cox, A. D. (1991) *Cancer 3*, 1–11.

Farnsworth, C. C., Kawata, M., Yoshida, Y., Takai, Y., Gelb, M. H., & Glomset, J. A. (1991) *Proc. Natl. Acad. Sci. U.S.A. 88*, 6196–6200.

Finegold, A. A., Johnson, D. I., Farnsworth, C. C., Gelb, M. H., Judd, S. R., Glomset, J. A., & Tamanoi, F. (1991) *Proc. Natl. Acad. Sci. U.S.A. 88*, 4448–4452.

Fukada, Y., Takao, T., Ohguro, H., Yoshizawa, T., Akino, T., & Shimonishi, Y. (1990) *Nature 346*, 658–660.

Gibbs, J. B. (1991) *Cell 65*, 1–4.

Glomset, J. A., Gelb, M. H., & Farnsworth, C. C. (1990) *Trends Biochem. Sci. 15*, 139–142.

Glomset, J. A., Gelb, M. H., & Farnsworth, C. C. (1991) *Curr. Opin. Lipidol. 2*, 118–124.

Gutierrez, L., & Magee, A. I. (1991) *Biochim. Biophys. Acta 1078*, 147–154.

Gutierrez, L., Magee, A. I., Marshall, C. J., & Hancock, J. F. (1989) *EMBO J. 8*, 1093–1098.

Hancock, J. F., Cadwallader, K., & Marshall, C. J. (1991) *EMBO J. 10*, 641–646.

Hrycyna, C. A., & Clarke, S. (1992) *J. Biol. Chem. 267*, 10457–10464.

Hrycyna, C. A., Sapperstein, S. K., Clarke, S., & Michaelis, S. (1991) *EMBO J. 10*, 1699–1709.

Khosravi, R., Lutz, R. J., Cox, A. D., Conroy, L., Bourne, J. R., Sinensky, M., Balch, W. E., Buss, J. E., & Der, C. J. (1991) *Proc. Natl. Acad. Sci. U.S.A. 88*, 6264–6268.

Kinsella, B. T., & Maltese, W. A. (1991) *J. Biol. Chem. 266*, 8540–8544.

Kohl, N. E., Diehl, R. E., Schaber, M. D., Rands, E., Soderman, D. D., He, B., Moores, S. L., Pompliano, D. L., Ferro-Novick, S., Powers, S., Thomas, K. A., & Gibbs, J. B. (1991) *J. Biol. Chem. 266*, 18884–18888.

Lai, R. K., Perez-Sala, D., Canada, F. J., & Rando, R. R. (1990) *Proc. Natl. Acad. Sci. U.S.A. 87*, 7673–7677.

Ma, Y.-T., & Rando, R. R. (1992) *Proc. Natl. Acad. Sci. U.S.A. 89*, 6275–6279.

Maltese, W. A. (1990) *FASEB J. 4*, 3319–3328.

Moores, S. L., Schaber, M. D., Mosser, S. D., Rands, E., O'Hara, M. B., Garsky, V. M., Marshall, M. S., Pompliano, D. L., & Gibbs, J. B. (1991) *J. Biol. Chem. 266*, 14603–14610.

Perez-Sala, D., Tan, E. W., Canada, F. J., & Rando, R. R. (1991) *Proc. Natl. Acad. Sci. U.S.A. 88*, 3043–3046.

Reiss, Y., Stradley, S. J., Gierasch, L. M., Brown, M. S., & Goldstein, J. L. (1991) *Proc. Natl. Acad. Sci. U.S.A. 88*, 732–736.

Rine, J., & Kim, S.-H. (1990) *New Biol. 2*, 219–226.

Seabra, M. C., Reiss, Y., Casey, P. J., Brown, M. S., & Goldstein, J. L. (1991) *Cell 65*, 429–434.

Sinensky, M., & Lutz, R. J. (1992) *BioEssays 14*, 25–31.

Stephenson, R. C., & Clarke, S. (1990) *J. Biol. Chem. 265*, 16248–16254.

Stephenson, R. C., & Clarke, S. (1992) *J. Biol. Chem. 267*, 13314–13319.

Tan, E. W., & Rando, R. R. (1992) *Biochemistry 31*, 5572–5578.

Volker, C., Lane, P., Kwee, C., Johnson, M., & Stock, J. (1991) *FEBS Lett. 295*, 189–194.

Yamane, H. K., Farnsworth, C. C., Xie, H., Howald, W., Fung, B. K.-K., Clarke, S., Gelb, M. H., & Glomset, J. A. (1990) *Proc. Natl. Acad. Sci. U.S.A. 87*, 5868–5872.

Yokoyama, K., Goodwin, G. W., Ghomashchi, F., Glomset, J. A., & Gelb, M. H. (1991) *Proc. Natl. Acad. Sci. U.S.A. 88*, 5302–5306.

Yoshida, Y., Kawata, M., Katayama, M., Horiuchi, H., Kita, Y., & Takai, Y. (1991) *Biochem. Biophys. Res. Commun, 175*, 720–728.